

ARTICLE

Supporting Information

Flexible, Adhesive and Self-Healable Hydrogel-based Wearable Strain Sensor for Human Motion and Physiological Signal Monitoring

Shan Xia, Shixin Song, Fei Jia*, Guanghui Gao*

Polymeric and Soft Materials Laboratory, School of Chemical Engineering and Advanced Institute of Materials Science, Changchun University of Technology, Changchun 130012, China

Corresponding authors: Fei Jia, Guanghui Gao

E-mail: jiafei@ccut.edu.cn (F. Jia); ghgao@ccut.edu.cn (G. Gao)

Table S1. Recipes for all hydrogel samples.

Hydrogels	NaCl (g)	SDS (g)	H ₂ O (mL)	AC (mL)	AAm (g)	LMA (μ L)	CS (mg)	c-MWCNT (mg)
HPAAm	0.15	0.3	15	15	3	37.5	0	0.0
HPAAm/CS	0.15	0.3	15	15	3	37.5	45	0.0
HPAAm/CS-C-MWCNT	0.15	0.3	15	15	3	37.5	45	22.5
0.1 mol%-LMA	0.15	0.3	15	15	3	12.5	45	22.5
0.2 mol%-LMA	0.15	0.3	15	15	3	25.0	45	22.5
0.3 mol%-LMA	0.15	0.3	15	15	3	37.5	45	22.5
0.4 mol%-LMA	0.15	0.3	15	15	3	50.0	45	22.5
0.5 mol%-LMA	0.15	0.3	15	15	3	62.5	45	22.5
0.5 wt%-CS	0.15	0.3	15	15	3	37.5	15	22.5
1.0 wt%-CS	0.15	0.3	15	15	3	37.5	30	22.5
1.5 wt%-CS	0.15	0.3	15	15	3	37.5	45	22.5
2.0 wt%-CS	0.15	0.3	15	15	3	37.5	60	22.5
2.5 wt%-CS	0.15	0.3	15	15	3	37.5	75	22.5
0.25 wt%-c-MWCNT	0.15	0.3	15	15	3	37.5	45	7.5
0.50 wt%-c-MWCNT	0.15	0.3	15	15	3	37.5	45	15.0
0.75 wt%-c-MWCNT	0.15	0.3	15	15	3	37.5	45	22.5
1.00 wt%-c-MWCNT	0.15	0.3	15	15	3	37.5	45	30.0



Figure S1. The dispersion of c-MWCNT and CS-c-MWCNT in acetic acid solution after standing for 15 days.

Figure S1 showed the dispersion of c-MWCNT and CS-c-MWCNT in acetic acid solution after standing for 15 days. Obviously, the stability of c-MWCNT was improved after adding CS into the acetic acid solution, indicating the strong electrical interaction between c-MWCNT and chitosan.

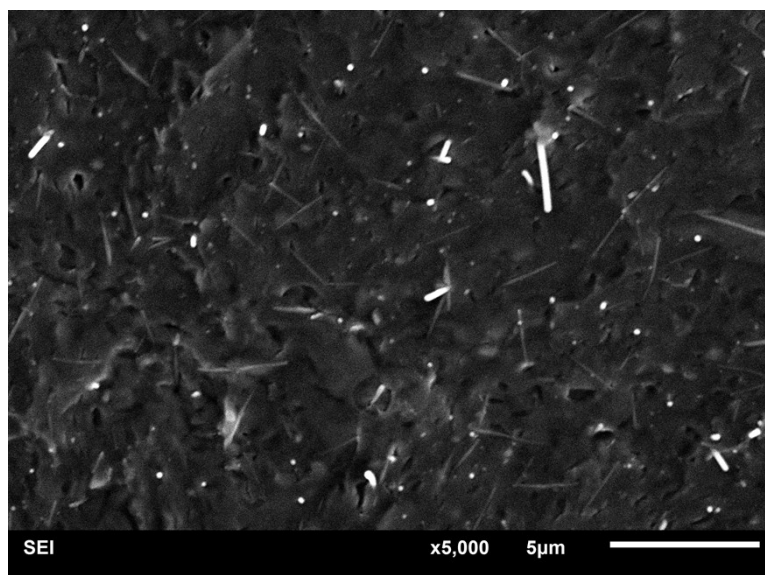


Figure S2. The SEM image of HPAAm/CS-c-MWCNT hybrid hydrogel.

Figure S2. showed the microstructure of the HPAAm/CS-c-MWCNT hybrid hydrogel after freeze-drying. It was clear that the c-MWCNT were uniformly dispersed in the hydrogel without any aggregation. In addition, c-MWCNT overlapped with each other in hydrogel to form a conductive network, which was beneficial to achieve tunable electromechanical behavior.

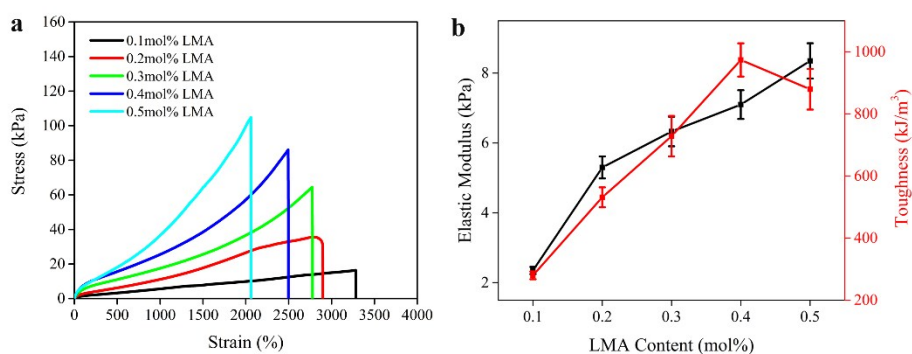


Figure S3. The tensile properties of HPAAm/CS-c-MWCNT hybrid hydrogels with different LMA content: a) stress-strain curves and b) the elastic modulus and toughness corresponding to a).

The effect of LMA content on the mechanical property of HPAAm/CS-c-MWCNT hybrid hydrogels was measured. As shown in Figure S3, with increasing the molar ratio of LMA to AAm from 0.1 mol % to 0.5 mol %, the fracture stress and elastic modulus of HPAAm/CS-c-MWCNT hydrogels considerably increased. It was because that the more hydrophobic segment could be stabilized by SDS and acted as hydrophobic cross-linking points to effectively dissipated energy to withstand external force, thus, resulting in HPAAm/CS-c-MWCNT hybrid hydrogels exhibited increasing mechanical strength. However, when the molar ratio of LMA to AAm increased from 0.4 mol % to 0.5 mol %, the toughness of HPAAm/CS-c-MWCNT hydrogel decreased obviously. It could be attributed that the excess LMA would induce inhomogeneity for the hydrogel network, consequently leading to the decrease of toughness.

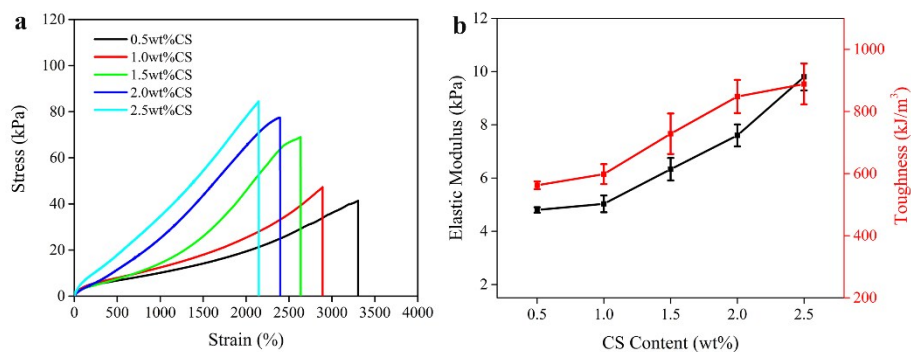


Figure S4. The tensile properties of HPAAm/CS-c-MWCNT hybrid hydrogels with different CS content: a) stress-strain curves and b) the elastic modulus and toughness corresponding to a).

As shown in Figure S4, the elastic modulus and toughness increased of hybrid hydrogel increased gradually as the CS content increased from 0.5 wt% to 2.5 wt%. This was due to the rigidity of the chitosan molecular chain, thus could as an enhanced network to effectively improve the mechanical strength of the hybrid hydrogel. On the other hand, chitosan could be used as a molecular scaffold to ensure the stability and integrity of the network structure of hydrogel when subjected to external forces, and ultimately improved the mechanical properties of the hybrid hydrogel.

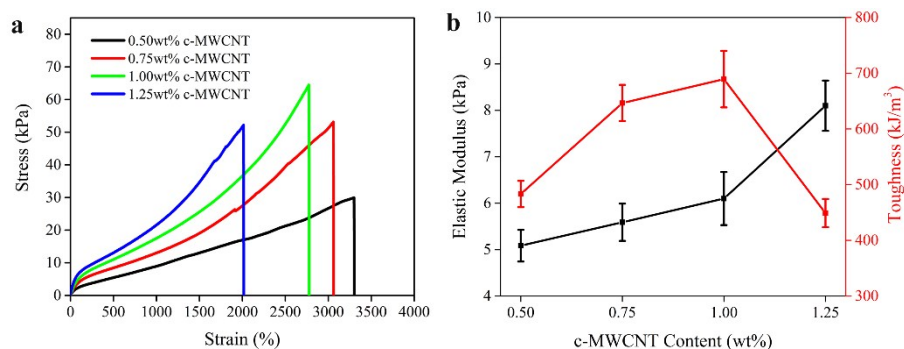


Figure S5. The tensile properties of HPAAm/CS-c-MWCNT hybrid hydrogels with different c-MWCNT content: a) stress-strain curves and b) the elastic modulus and toughness corresponding to a).

The effect of c-MWCNT content on the mechanical property of HPAAm/CS-c-MWCNT hybrid hydrogels was also measured. As shown in Figure S5, the elastic modulus of hybrid hydrogels increased gradually as the content of c-MWCNT increased. The fracture stress and toughness increased with increasing c-MWCNT contents from 0 to 1.0 wt%, and then decreased at a c-MWCNT content of 1.25 wt%. Since the c-MWCNT was a kind of hard carbon-based material, introducing it into the hydrogel through electrostatic interaction to form an enhanced network could effectively improve the mechanical strength of the hybrid hydrogel. However, as the c-MWCNT further increased from 1.0 wt% to 1.25 wt%, the excess c-MWCNT tended to aggregate, resulting in an inhomogeneous network structure and reduced mechanical properties of hybrid hydrogel.

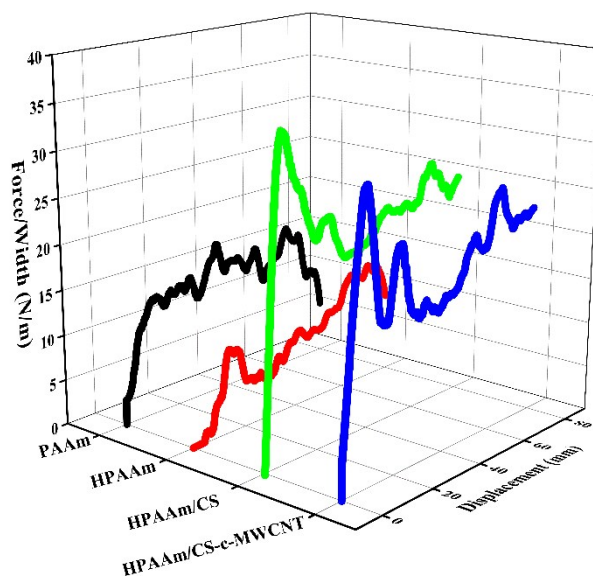


Figure S6. The peeling curves of PAAm, HPAAm, HPAAm/CS and HPAAm/CS-c-MWCNT hybrid hydrogels on aluminum substrates.

As shown in Figure S6, the PAAm/CS and PAAm/CS-c-MWCNT hydrogels exhibited enhanced adhesive properties than PAAm and PAAm/CS hydrogels after adding CS into hydrogel, indicating that the introduction of CS could improve the adhesion of hydrogel.

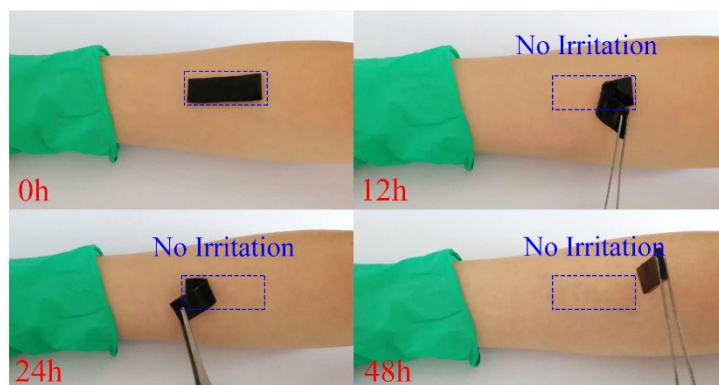


Figure S7. The photographs of volunteer arm after contacted with hydrogel for different time.

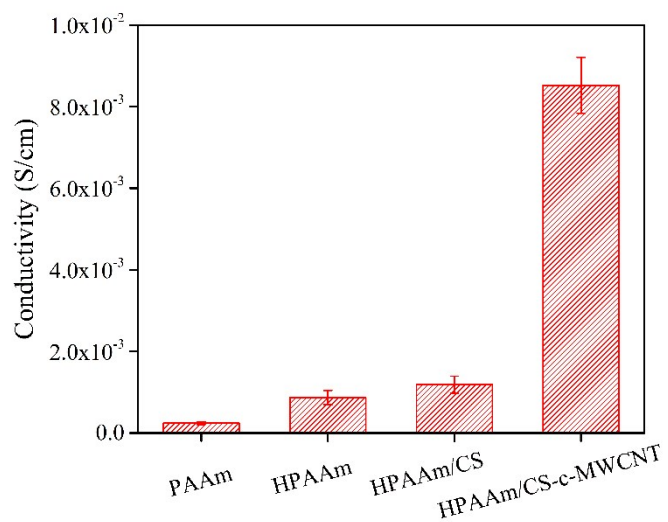


Figure S8. The conductivity of PAAm hydrogel, HPAAm hydrogel, HPAAm/CS hydrogel and HPAAm/CS-c-MWCNT hybrid hydrogel.

The conductivity of PAAm, HPAAm, HPAAm/CS, HPAAm/CS-c-MWCNT hybrid hydrogels were shown in Figure S8. It was clearly that the HPAAm/CS-c-MWCNT hybrid hydrogel exhibited the highest conductivity due to the introduction of c-MWCNT, which could overlap with each other to construct the conductive pathway.

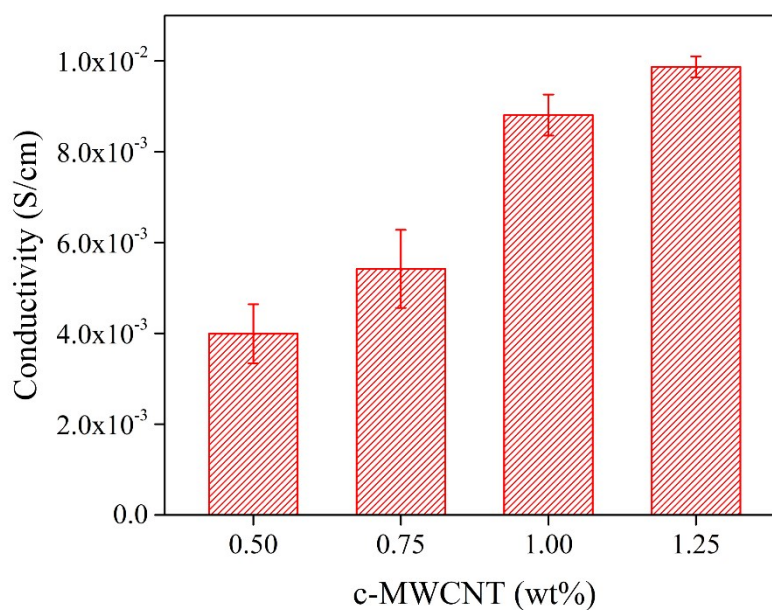


Figure S9. The conductivity of HPAAm/CS-c-MWCNT hybrid hydrogel with different content of c-MWCNT.

As shown in Figure S9, the conductivity of HPAAm/CS-c-MWCNT hybrid hydrogel increased gradually as increasing c-MWCNT content. It indicated that the addition of c-MWCNT played a key role in the conductivity of the hydrogel. Considering the combination of mechanical properties of hydrogel, a subsequent series of experiments was carried out using a formula with c-MWCNT and LMA content of 1.00 wt% and 0.3 mol%, respectively.

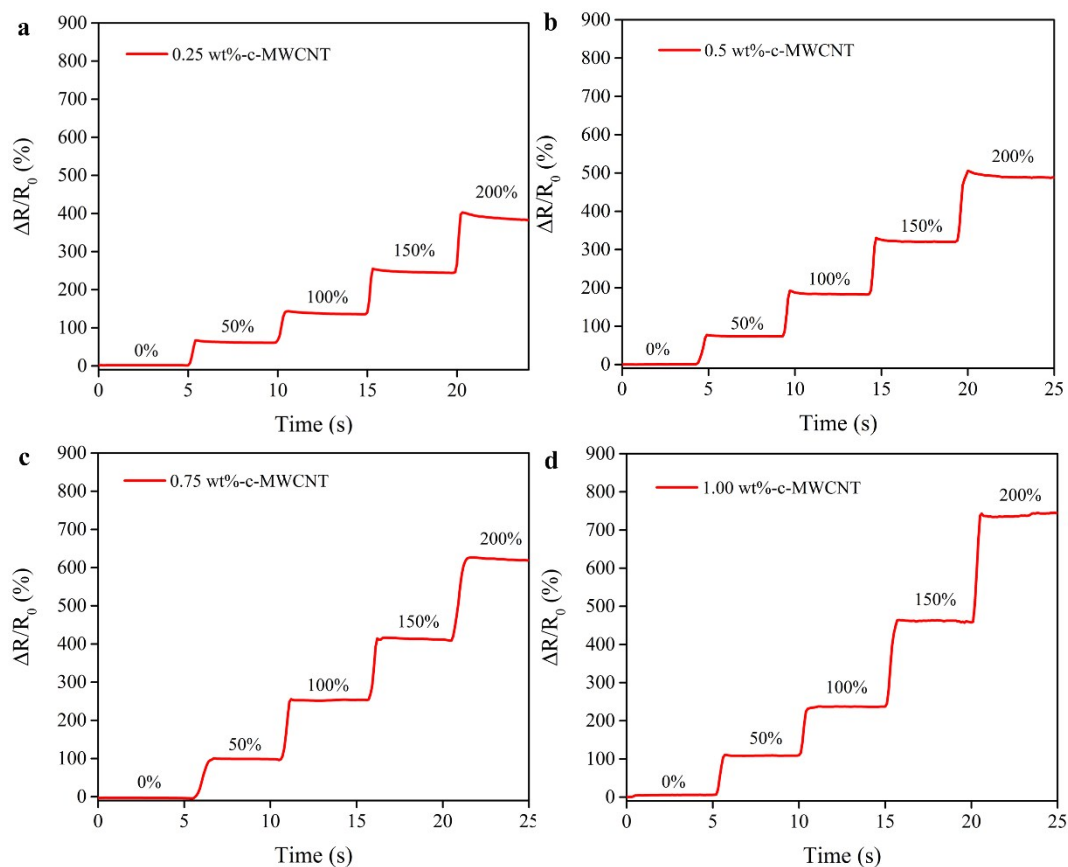


Figure S10. The strain sensitive resistance variations of HPAAm/CS-c-MWCNT hybrid hydrogel with different content of c-MWCNT.

As shown in Figure S10, four HPAAm/CS-c-MWCNT hybrid hydrogels exhibited excellent strain sensitive resistance variations. As the elongation increased step by step, the resistance increased with a step-like trend. When the hydrogel was in a stretch-holding state, the resistance could also be stabilized at a fixed value. Therefore, the elongation of the hydrogel could be accurately judged based on the degree of resistance variation. Moreover, HPAAm/CS-c-MWCNT hybrid hydrogels displayed significantly enhanced strain-sensitive resistance variations with increasing c-MWCNT content.

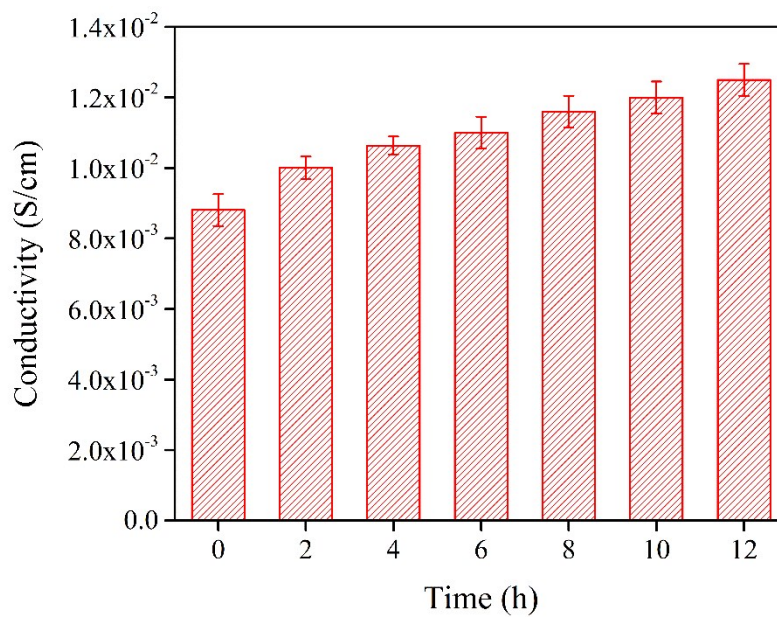


Figure S11. The conductivity of HPAAm/CS-c-MWCNT hybrid hydrogel after placing in open air for different time.

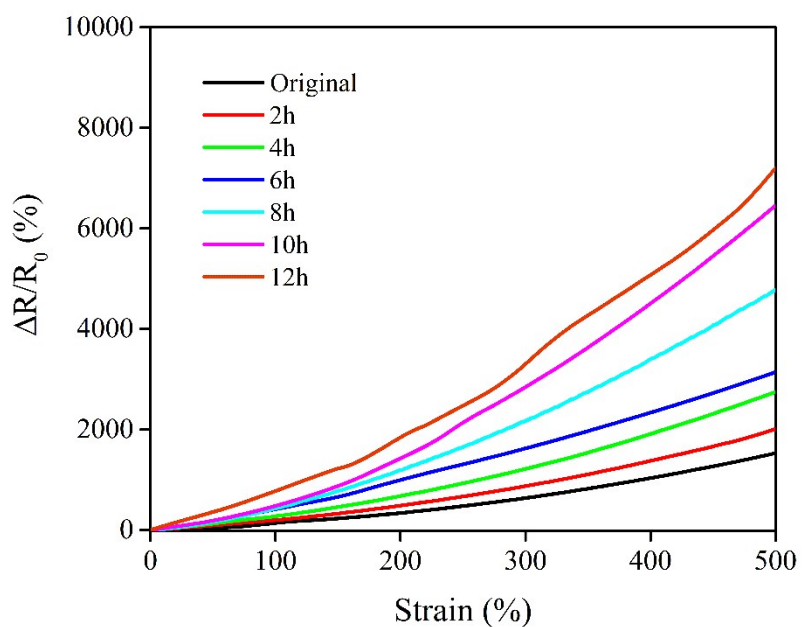


Figure S12. The sensitivity of HPAAm/CS-c-MWCNT hybrid hydrogel sensor after placing in open air for different time.

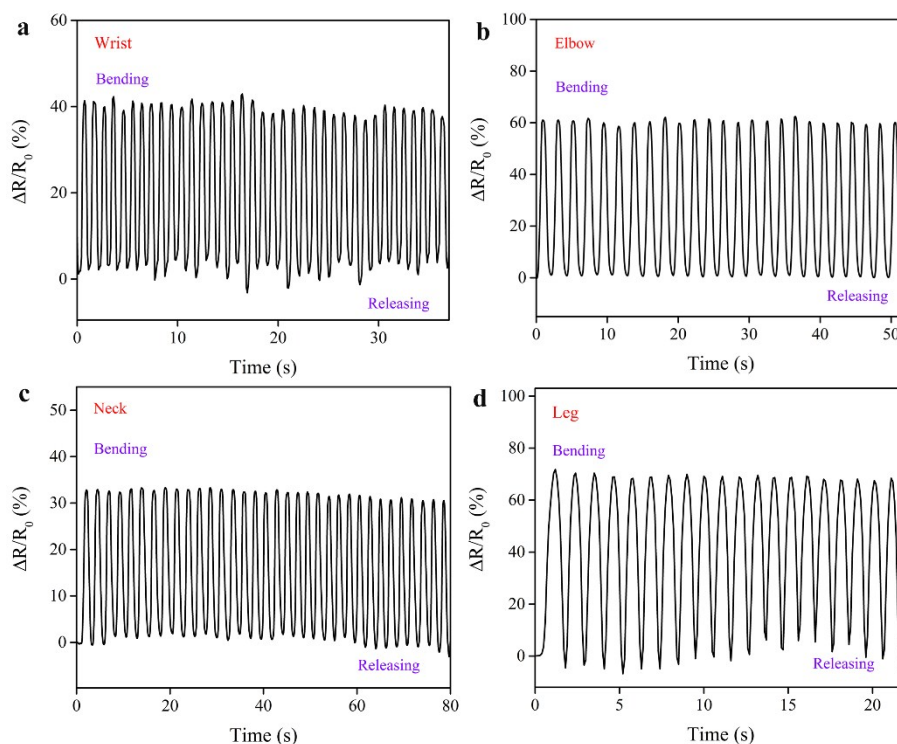


Figure S13. The recorded resistance variations the hydrogel strain sensor in response to different joints motions.

Figure S13 illustrated the relative resistance variations during consecutive bending and releasing cycles for hybrid hydrogel strain sensors integrated to wrist, elbow, neck, and knee joint. It was obvious that hybrid hydrogel sensor exhibited repeatable and high sensitivity without any apparent loss in the resistance even after consecutive cycles, indicating the excellent durability and stability of hydrogel in electromechanical behavior.

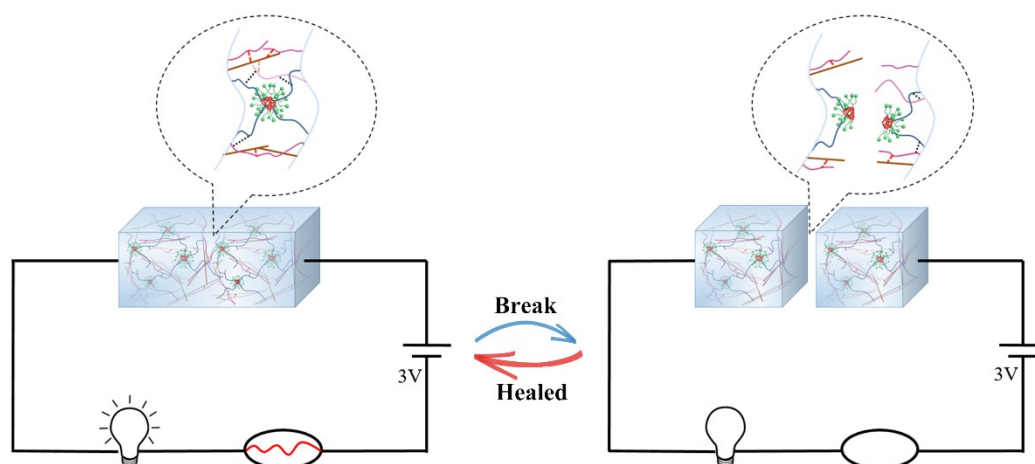


Figure S14. The self-healing mechanism of hybrid hydrogel.

For the hybrid hydrogels consisting of dynamic cross-linking network, both hydrophobic association, electrostatic interaction and hydrogen bonding might contribute to the self-healing behavior. The self-healing mechanism of hybrid hydrogel was shown in Figure S14. When the fracture surfaces of hybrid hydrogel were brought into contact, the broken hydrophobic association on the cut surfaces could reform over time. While the electrostatic interaction and the hydrogen bonds could also reformed and stabilized the reformed hydrophobic association. The synergistic interaction of hydrophobic association, electrostatic interaction and hydrogen bonding contributed to the self-healing properties of the hybrid hydrogel, which restored the mechanical and electrical properties of the hybrid hydrogel.

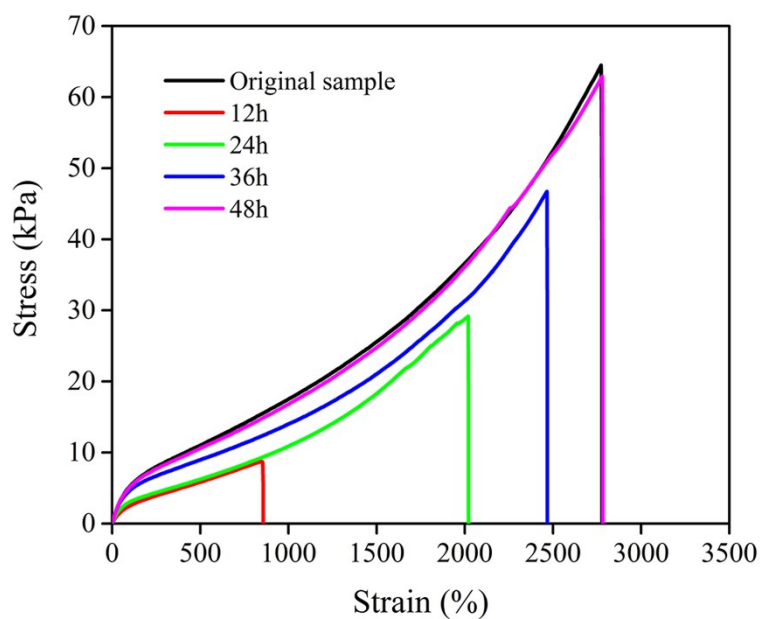


Figure S15. The tensile curves of hybrid hydrogel as the healing time extend.

As shown in Figure S15, as healing time extended, the tensile property of hydrogel gradually recovered. After a healing time of 48h, the strength of self-healed hydrogel reached to 100% of that of pristine hydrogel, which also demonstrated the recombination of the dynamic cross-linking network inside the hydrogel.

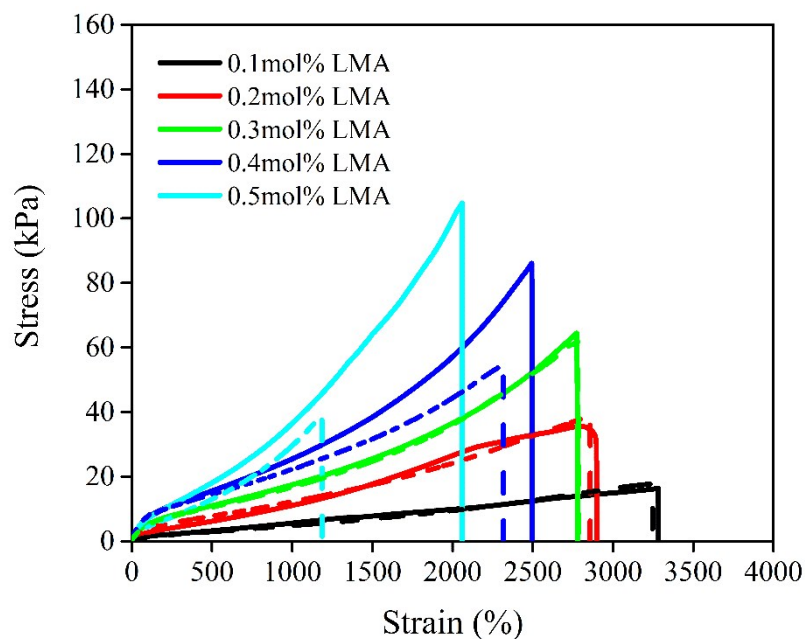


Figure S16. The effect of LMA content on self-healing behavior of hybrid hydrogels. The solid and dashed lines represented the tensile curves of the hybrid hydrogel before and after healing 48 h, respectively.

As shown in Figure S16, when healing time was 48 h, the tensile properties of hybrid hydrogels with 0.1, 0.2 and 0.3 mol% LMA could completely reach that of pristine hydrogels. However, as the LMA content further increased, the healing efficiency of the hydrogel reduced. It was because that as the LMA content increased, the cross-linking density in the hydrogel also increased, resulting in hindered movement of the hydrophobic segment of the fracture surface and a reduced ability to self-heal.